Int. J. Heat Mass Transfer. Vol. 31, No. 3, pp. 660–663, 1988
Printed in Great Britain

0017–9310/88 $3.00+0.00
Pergamon Press plc

Local heat transfer from a horizontal cylinder in unstratified and salt-stratified fluid layers

D. G. NEILSON and F. P. INCROPERA
Heat Transfer Laboratory, School of Mechanical Engineering, Purdue University, W. Lafayette, IN 47907, U.S.A.

(*Received* 25 *May* 1987 *and in final form* 28 *August* 1987)

THE PROBLEM of heat transfer from a horizontal cylinder in a quiescent fluid has been widely studied for a variety of special cases. For an infinite ambient, a free convection boundary layer develops around the cylinder, feeding a plume which ascends above the cylinder, and reliable convection correlations have been established [1]. For a finite liquid ambient with a free air–liquid interface, deflection and cooling of the plume at the interface induces a recirculating flow which significantly enhances heat transfer from the cylinder [2–4]. If the ambient is thermally stratified, vertical plume growth is restrained and, again, there is enhancement of convection heat transfer from the cylinder [5]. In contrast, if the ambient is solutally stratified, plume growth is restrained but there is suppression of convection heat transfer [6, 7].

Despite the considerable interest in free convection from horizontal cylinders, most experimental studies have been performed for isothermal surfaces and, hence, have been unable to yield results for the local convection coefficient. If, instead, a uniform surface heat flux is imposed, variations in the local coefficient may be determined. Such variations may be significant as, for example, in a solutally stratified fluid where multiple, recirculating layers are known to develop about the cylinder [7]. Existing studies appear to be limited to a large, unstratified ambient for which predictions [8] and experiments [9] have been performed at Prandtl numbers of 1 and approximately 1000, respectively. The purpose of this study is to obtain local measurements in unstratified water ($Pr \approx 6$) and in a salt-stratified solution for which flow around the cylinder is strongly influenced by the stratification.

Experiments were performed in a cubical test cell the interior dimensions of which measured 304.8 mm on a side. A 304.8 mm long, 25.1 mm diameter cylindrical heat source was inserted through holes drilled in opposing sidewalls, with the centerline maintained 38.1 mm above the test cell bottom. As shown in Fig. 1, a single sheet of 2 mil stainless steel foil was bonded to a bakelite tube and electrically coupled (through spot welds and copper paint) to copper busbars at each end. To minimize upstream disturbances in boundary layer development, the cylinder was oriented with the seam of the wrapped foil positioned at or near the top of the cylinder ($\theta \approx \pi/2$). Power to the foil was provided by a d.c. supply, and the foil voltage drop and current were measured. The existence of uniform heat dissipation in the foil was confirmed by the measurement of uniform and linear voltage distributions in the circumferential and axial directions, respectively.

Foil temperatures at the midplane of the tube were sensed to 0.10°C accuracy by twelve calibrated copper–constantan thermocouples placed at 30° increments around the circumference. The thermocouple junctions were inserted through holes in the bakelite and were epoxied flush with the outer surface of the tube. Lead wires were accessed through the tubing. A thin coating of polytetrafluoroethylene (PTFE) was applied to the outer surface of the foil to protect it from the saline environment. The temperature measurements were corrected for the drop across the coating (≈ 0.25°C) to determine the true surface temperature. The local Nusselt number $Nu(\theta)$ could then be determined from knowledge of the local surface and ambient temperatures. The ambient temperature was measured at the level of and at a lateral distance of 152 mm from the cylinder centerline.

The existence of a uniform surface heat flux was confirmed

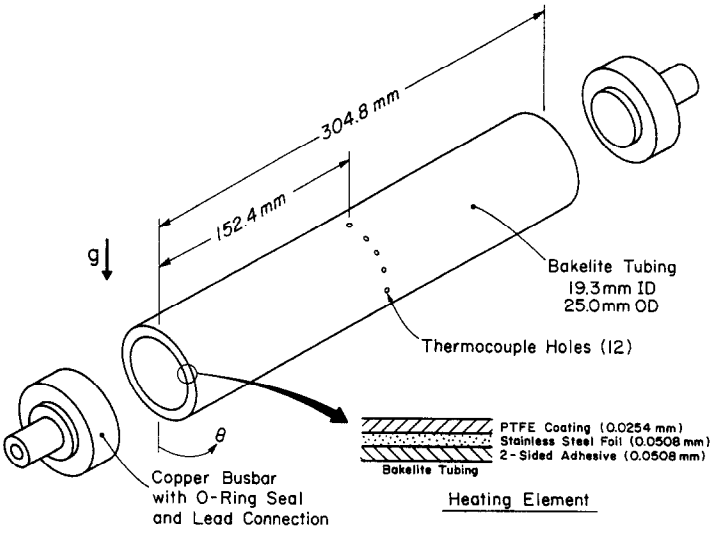

FIG. 1. Schematic of heated cylinder.

NOMENCLATURE

D	cylinder diameter
g	gravitational acceleration
k	thermal conductivity
m_s	salt mass fraction
N	stratification parameter, $-\beta_s(dm_s/dz)D/\beta_T(\bar{T}_s - T_\infty)_{max}$
Nu	local Nusselt number, $qD/k[T_s(\theta) - T_\infty]$
q	surface heat flux
Ra^*	modified Rayleigh number, $g\beta_T qD^4/\alpha\nu k$
t	time
T_s	local surface temperature
$\bar{T}_s$	circumferential average surface temperature
T_∞	ambient temperature.

Greek symbols

α	thermal diffusivity
β_s	solutal expansion coefficient
β_T	thermal expansion coefficient
θ	polar angle
ν	kinematic viscosity.

by performing a two-dimensional (r, θ) conduction analysis on a composite of the foil/PTFE coating. The inner surface of the foil and the ends of the composite ($\theta = 0, \pi$ rad) were assumed to be adiabatic, while convection heat transfer was allowed to occur from the outer surface of the PTFE to the fluid. The imposed circumferential distribution of the convection coefficient, $h(\theta)$, corresponded to worst cast experimental conditions for which the variation of h with θ was most pronounced. Uniform ohmic dissipation in the stainless steel foil was imposed, and the resulting variation in the local heat flux at the outer surface of the coating, $q(\theta)$, was calculated. The circumferential heat flux distribution was then utilized to adjust $h(\theta)$, and the calculations were repeated. This iterative process confirmed that the heat flux was uniform to within 1% over most of the surface ($0 \leqslant \theta < 170°$) and that the maximum deviation, which occurred at the top of the cylinder ($\theta = 180°$), was less than 3%.

Experimental conditions were differentiated in terms of a modified Rayleigh number, Ra^*, based on the surface heat flux and a stratification parameter, N, which measures the stabilizing effect of a solutally stratified ambient relative to the destabilizing effect of the heated cylinder. In the definition of N, dm_s/dz is the initial salt concentration gradient imposed on the ambient and $(\bar{T}_s - T_\infty)_{max}$ is the maximum average surface to ambient temperature difference recorded during an experiment. For saline water, thermophysical properties were evaluated from tabulated data [10] using the mean temperature, $(\bar{T}_s + T_\infty)/2$, and the initial salt mass fraction at the cylinder midheight.

Four experiments were performed, two each for unstratified ($N = 0$) and stratified ($N = 1.1, 1.9$) conditions. Each of the stratified cases corresponded to an initial salinity gradient of -11.0% m^{-1}. For the stratified and unstratified conditions, experiments were performed for heat fluxes of 515 and 1565 W m^{-2}, which provided Rayleigh numbers

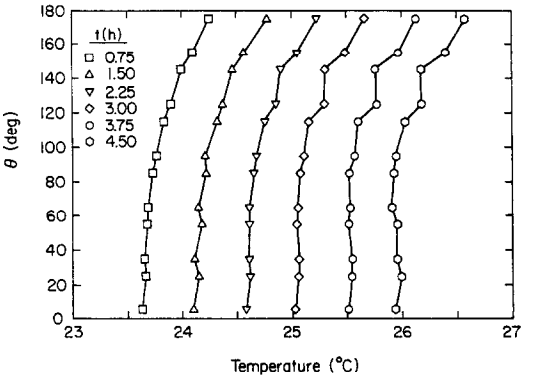

FIG. 2. Circumferential variations of cylinder surface temperature for $N = 0$ and $Ra^* = 6.2 \times 10^6$.

(based on initial conditions) of approximately 6.5×10^6 and 2.0×10^7, respectively.

The circumferential variation in the cylinder surface temperature is shown in Fig. 2 for selected times during the experiment for which $N = 0$ and $Ra^* = 6.2 \times 10^6$. Assuming symmetry about the vertical midplane, measurements obtained on opposite sides of the midplane have been combined to yield a single plot for $0 \leqslant \theta \leqslant 180°$. With increasing θ from the stagnation point, T_s increases gradually up to $\theta \approx 100°$ and more sharply for $\theta \gtrsim 100°$. The sharper increase may be due to enhanced thickening of the thermal boundary layer as the top of the cylinder is approached and/or flow disturbances induced by the foil seam. The profile distortion associated with large θ and t may be due to developing asymmetries and/or bubbles which appeared near the top of the cylinder toward the end of the experiment.

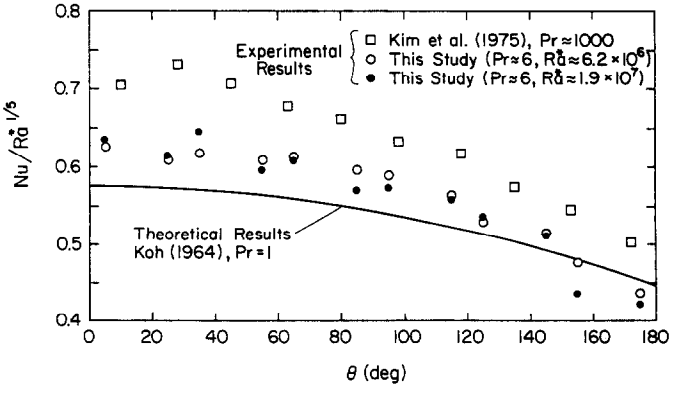

FIG. 3. Circumferential variations in local Nusselt number for unstratified conditions ($N = 0$).

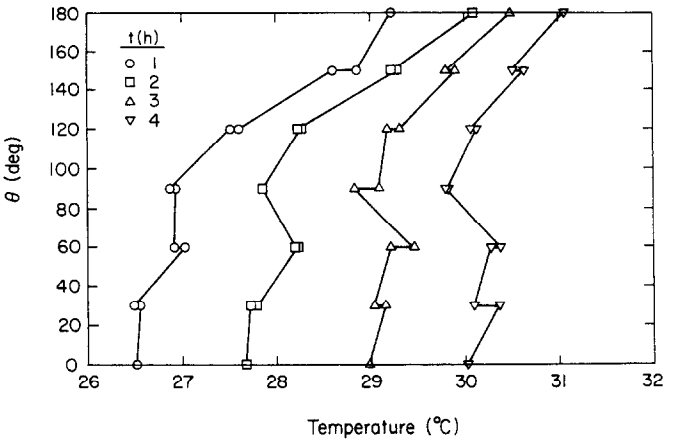

FIG. 4. Circumferential variations of cylinder surface temperature for $N = 1.9$ and $Ra^* = 6.9 \times 10^6$.

In the experiments performed for $N = 0$, a steady-state condition was achieved and the corresponding Nusselt number distributions are shown in Fig. 3. Data from this study are contrasted with a boundary layer solution [8], which is valid for $\theta \lesssim 115°$, and with data obtained for mineral oil [9]. Although results are normalized with respect to $Ra^{*1/5}$, there remains a clear Prandtl number dependence. This behavior is not unexpected in view of the large Prandtl number range, and the trend of increasing Nu with increasing Pr is consistent with results for an isothermal cylinder [11]. Data for the two Rayleigh numbers of this study are in good agreement, and the trend of decreasing Nu with increasing θ is consistent with the previous results [8, 9]. The crossover between the data of this study and the analytical results of Koh [8] at $\theta \approx 150°$ may be due to disturbances related to the foil seam and/or to a breakdown in the Koh model for large θ.

With salt stratification, circumferential variations in T_s are more pronounced, and representative results are shown in Fig. 4 for the first 4 h of the experiment corresponding to $N = 1.9$ and $Ra^* = 6.9 \times 10^6$. For these experiments the cylinder was oriented with single thermocouples at $\theta = 0$ and 180° and with two thermocouples symmetrically positioned on opposite sides of the midplane for the intermediate values of θ. Although there is some scatter to the data, a distinguishing feature of the results between $t = 1$ and 3 h is the temperature inversion which occurs between 30 and 90°. For this time interval flow visualization performed using the shadowgraph technique (Figs. 5(a) and (b)) revealed the existence of a diffusive interface (dark band) attached to the cylinder at $\theta \approx 65°$. Such interfaces, which separate mixed layers (gray regions) driven by thermal buoyancy, are characteristic of double-diffusive convection around a heated cylinder, and their temperal behavior has been extensively described for an isothermal cylinder [7]. In this case the boundary layer which develops at the bottom of the cylinder is impeded by the interface, and the flow is deflected horizontally to establish a bottom recirculating layer. The 'barrier' provided by the interface allows a second boundary layer to form, beginning at the interface and extending to the top of the cylinder. Recirculating motion in each of the two layers is analogous to buoyancy induced flow in a rectangular cavity with differentially heated sidewalls. Temperatures sensed on the cylinder at locations below and above the attached interface reveal the nature of local thermal conditions. The temperature is discernibly larger just beneath the attached interface, where fluid heated by the cylinder is turned toward the sidewall. In contrast, above the interface, the cylinder is cooled by fluid moving toward the heat source from the sidewall. The attached interface is eroded after

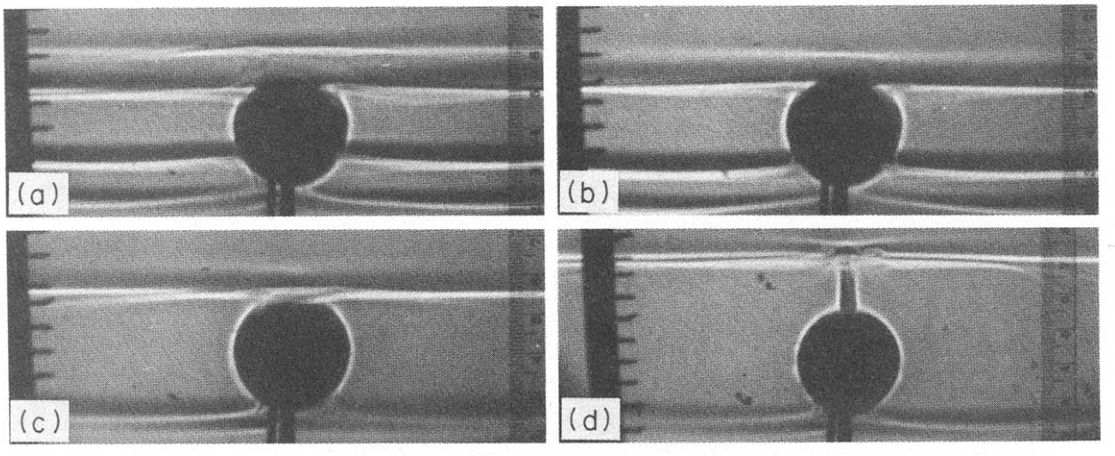

FIG. 5. Shadowgraph images of diffusive interfaces and mixed layers around a heated cylinder in a salt-stratified solution ($N = 1.9$, $Ra^* = 6.9 \times 10^6$): (a) $t = 2$ h; (b) $t = 3$ h; (c) $t = 8$ h; (d) $t = 23$ h.

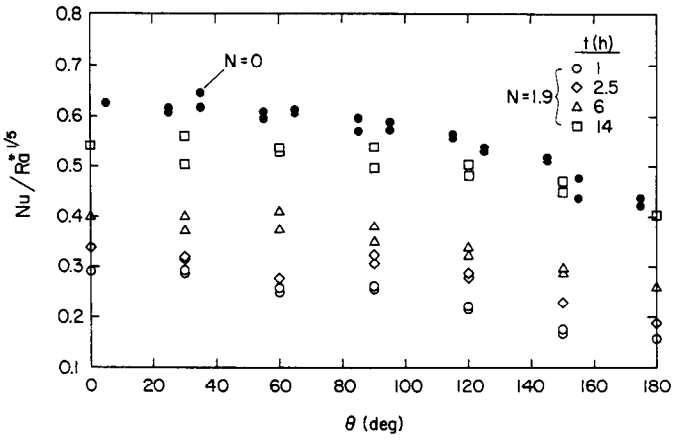

FIG. 6. Circumferential variation in local Nusselt number for unstratified conditions and at selected times for stratified conditions ($n = 1.9$, $Ra^* = 6.9 \times 10^6$).

approximately 8 h (Fig. 5(c)), leaving a single recirculating layer between interfaces at the top and bottom of the cylinder. Subsequently, the layer grows with time, as a vertical plume ascends above the cylinder (Fig. 5(d)). For $T \gtrsim 8$ h, T_s decreases monotonically with increasing θ, and the circumferential distribution resembles results obtained for $N = 0$ (Fig. 2).

Local Nusselt number distributions obtained at selected times for $N = 1.9$ and $Ra^* = 6.9 \times 10^6$ are contrasted with results for unstratified conditions in Fig. 6. During the early stages of the experiment, the effect of the diffusive interface at $\theta \approx 65°$ is revealed by the minimum corresponding to $Nu(\theta = 60°)$ at $t = 2.5$ h. In addition for all values of θ, heat dissipation is inhibited by the stratified conditions and $Nu(\theta)$ is substantially less than results for $N = 0$. With increasing t, however, degradation of the diffusive interface, onset of the vertical plume, and growth of the mixed layer about the cylinder cause $Nu(\theta)$ to approach the limiting results for $N = 0$.

For $N = 1.1$ and $Ra^* = 2.2 \times 10^7$, stratification was sufficiently weak to preclude attachment of a diffusive interface to the cylinder. At the onset of heating, a single mixed layer developed around the cylinder, and throughout the experiment circumferential distributions of T_s and Nu were similar to those determined for $N = 0$. Once again, $Nu(\theta)$ was substantially less than results for $N = 0$ during the early stages of the experiment but approached the $N = 0$ limit with increasing time.

In conclusion, it may be said that, in an unstratified ambient, the circumferential variation of the local Nusselt number is characterized by a monotonic decay from a maximum value associated with the lower stagnation point. In contrast, if the ambient is solutally stratified, double-diffusive interfaces may attach to the cylinder, inducing local minima in $Nu(\theta)$. However, with increasing time, the interfaces erode, causing a single mixed layer to develop around the cylinder and $Nu(\theta)$ to approach results corresponding to $N = 0$.

Acknowledgement—Support of this work by the National Science Foundation under Grant No. CBT-8316580 is gratefully acknowledged.

REFERENCES

1. V. T. Morgan,The overall convective heat transfer from smooth circular cylinders. In *Advances in Heat Transfer* (Edited by T. F. Irvine and J. P. Hartnett), pp. 199–264. Academic Press, New York (1975).
2. G. F. Masters, Natural convection heat transfer from a horizontal cylinder in the presence of nearby walls, *Can. J. Chem. Engng* **53**, 144–149 (1977).
3. F. P. Incropera and M. A. Yaghoubi, Free convection heat transfer from heated cylinders immersed in a shallow water layer, *J. Heat Transfer* **101**, 743–745 (1979).
4. F. P. Incropera and M. A. Yaghoubi, Buoyancy driven flows originating from heated cylinders in a finite water layer, *Int. J. Heat Mass Transfer* **23**, 269–278 (1980).
5. R. Eichhorn, J. H. Lienhard and C.-C. Chen, Natural convection from isothermal spheres and cylinders immersed in a stratified fluid, *Proc. 5th International Heat Transfer Conference*, Tokyo, Japan, NC1.3, pp. 10–14 (1974).
6. B. Gebhart and R. H. Hubbell, Transport processes induced by a heated horizontal cylinder submerged in quiescent, salt-stratified water, *Proc. 24th Heat Transfer and Fluid Mechanics Institute*, Corvallis, Oregon, pp. 203–219 (1979).
7. D. G. Neilson and F. P. Incropera, Double-diffusive flow and heat transfer for a cylindrical source submerged in a salt-stratified solution, *Int. J. Heat Mass Transfer* **30**, 2559–2570 (1987).
8. J. C. Y. Koh, Laminar free convection from a horizontal cylinder with prescribed surface heat flux, *Int. J. Heat Mass Transfer* **7**, 811–823 (1964).
9. C. B. Kim, T. J. Pontikes and D. E. Wollersheim, Free convection from a horizontal cylinder with isothermal and constant heat flux surface conditions, *J. Heat Transfer* **97**, 129–130 (1975).
10. United States Office of Saline Water, Technical Data Book (1964).
11. S. W. Churchill and H. H. S. Chu, Correlating equations for laminar and turbulent free convection from a horizontal cylinder, *Int. J. Heat Mass Transfer* **18**, 1049–1056 (1975).